

Enhancement of Ionization Efficiency by Electrochemical Reaction Products in On-Line Electrochemistry/Electrospray Ionization Fourier Transform Ion Cyclotron Resonance Mass Spectrometry

Tianyi Zhang, Sergiu P. Palii, John R. Eyler, and Anna Brajter-Toth*

Department of Chemistry, University of Florida, P.O. Box 117200, Gainesville, Florida 32611-7200

A miniaturized two-electrode electrochemical (EC) cell was developed and was coupled on-line with an electrospray ionization Fourier transform ion cyclotron resonance mass spectrometer (ESI-FTICR MS). Electrochemistry on-line with mass spectrometry, EC/ESI-FTICR MS, of triphenylamine (TPA), which undergoes one-electron oxidation to form a radical cation (TPA^{•+}), demonstrates a significant sensitivity enhancement compared to ESI-FTICR MS. The on-line EC cell configuration with a stainless steel ES needle as the working electrode produces the highest sensitivity in EC/ESI-MS. The results provide evidence that, during the ES ionization, electrolytic reactions occur mainly in the ES tip region, as previously predicted. The results demonstrate that ESI-MS signal suppression by tetrabutylammonium perchlorate electrolyte, which can be a problem, is minimized in EC/ESI-MS. TPA^{•+} dimer tetraphenylbenzidine (TPB) can be detected by EC/ESI-MS, together with TPA^{•+}, as TPB^{•+} and TPB²⁺. The high mass resolving power of FTICR MS was exploited to identify TPB²⁺ dication in the presence of [TPA^{•+} - H]⁺ ions of the same *m/z*, from their respective isotopic distributions. The dimer dication TPB²⁺ can be detected only in EC/ESI-MS.

On-line combination of electrochemistry (EC) and mass spectrometry (MS), EC/MS, is an excellent tool for probing electron-transfer chemistry in solution in close to real time.¹ In most recent developments in EC/MS, several research groups have reported the use of an electrospray ionization (ESI) interface for coupling of electrochemistry to mass spectrometry.^{2–10} ESI is a soft ionization method, which operates at atmospheric pressure

and uses an electrostatic spray process to transfer preformed ions from solution into the gas phase. Ionization of neutral compounds can be accomplished by ESI.^{11–15}

Electrospray interface has been recognized as an electrolytic cell by Kebarle's group¹¹ and has been characterized as a controlled-current electrolytic cell by Van Berkel and Zhou.^{16,17} The electrolytic ionization in ES has been reported to be limited to compounds with the oxidation potential below 1 V that are stable in solution after the oxidation.^{3,12,13,17} As a result, coupling of an external electrochemical cell to the ES ion source can enhance the ion signal in EC/ESI-MS.^{2–7} An interesting result was reported recently by Johnson and co-workers, who showed that in EC/ESI-MS charge states that were generated by the electrochemical reduction of a metalloprotein did not change as a result of the electrolytic processes during the ESI.¹⁸

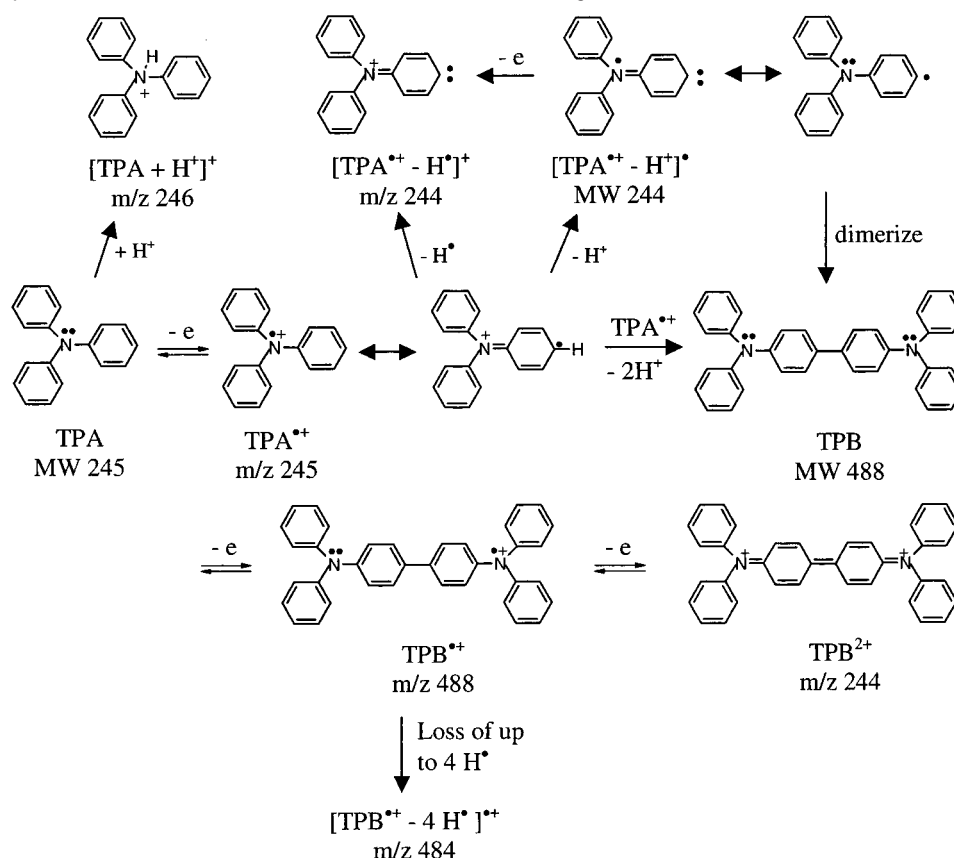
To achieve high efficiency of electrolysis in EC/MS, a fast response time, or both, EC cells of different designs, such as tubular-electrode cells,^{2,3,5,18} thin-layer flow cells,^{5,8} and porous flow-through cells,^{5,9,10} have been used. Unique problems encountered in coupling an EC cell to the ES ion source include high-voltage hazard, from the high ESI voltage, and possible interference with the EC cell voltage. Severe signal attenuation⁵ by common electrolytes that are used in electrochemistry, such as tetrabutylammonium perchlorate (TBAP) and tetrabutylammonium hexafluorophosphate (Bu₄NPF₆), has also been reported.^{2,3,19–21} Sup-

* Corresponding author: (phone) 352-392-7972; (fax) 352-392-4651; (e-mail) atoth@chem.ufl.edu.

- (1) Volk, K. J.; Yost, R. A.; Brajter-Toth, A. *Anal. Chem.* **1992**, *64*, 21A–33A.
- (2) Bond, A. M.; Colton, R.; D'Agnostino, A.; Downard, A. J.; Traeger, J. C. *Anal. Chem.* **1995**, *67*, 1691–1695.
- (3) Xu, X.; Lu, W.; Cole, R. B. *Anal. Chem.* **1996**, *68*, 4244–4253.
- (4) Lu, W.; Xu, X.; Cole, R. B. *Anal. Chem.* **1997**, *69*, 2478–2484.
- (5) Zhou, F.; Van Berkel, G. J. *Anal. Chem.* **1995**, *67*, 3643–3649.
- (6) Deng, H. T.; Van Berkel, G. J. *Anal. Chem.* **1999**, *71*, 4284–4293.
- (7) Pretty, J. R.; Deng, H. T.; Goeringer, D. E.; Van Berkel, G. J. *Anal. Chem.* **2000**, *72*, 2066–2074.
- (8) Deng, H. T.; Van Berkel, G. J. *Electroanal.* **1999**, *11*, 857–865.

- (9) Arakawa, R.; Abura, T.; Fukuo, T.; Horiguchi, H.; Matsubayashi, G. *Bull. Chem. Soc. Jpn.* **1999**, *72*, 1519–1523.
- (10) Juvra, U.; Wikstrom, H. V.; Bruins, A. P. *Rapid Commun. Mass Spectrom.* **2000**, *14*, 529–533.
- (11) Blades, A. T.; Ikonou, M. G.; Kebarle, P. *Anal. Chem.* **1991**, *63*, 2109–2114.
- (12) Van Berkel, G. J.; McLuckey, S. A.; Glish, G. L. *Anal. Chem.* **1992**, *64*, 1586–1593.
- (13) Xu, X.; Nolan, S. P.; Cole, R. B. *Anal. Chem.* **1994**, *66*, 119–125.
- (14) McCarty, T. C.; Lufaso, M. W.; Curtin, L. S.; McCarty, R. L. *J. Phys. Chem. B* **1998**, *102*, 10078–10086.
- (15) Schoener, D. F.; Olsen, M. A.; Cummings, P. G.; Basic, C. *J. Mass. Spectrom.* **1999**, *34*, 1069–1078.
- (16) Van Berkel, G. J.; Zhou, F. *Anal. Chem.* **1995**, *67*, 2916–2923.
- (17) Van Berkel, G. J.; Zhou, F. *Anal. Chem.* **1995**, *67*, 3958–3964.
- (18) Johnson, K. A.; Shira, B. A.; Anderson, J. L.; Amster, I. J. *Anal. Chem.* **2001**, *73*, 803–808.
- (19) Tang, L.; Kebarle, P. *Anal. Chem.* **1993**, *65*, 3654–3668.
- (20) Kebarle, P.; Tang, L. *Anal. Chem.* **1993**, *65*, 972A–986A.
- (21) Fenn, J. B. *J. Am. Soc. Mass. Spectrom.* **1993**, *4*, 524–535.

Scheme 1. Proposed Oxidation and Ion Formation Pathways of TPA^a



^a TPA^{•+} ion radical may also couple with neutral TPA.²⁹

pression of the EC/ESI-MS signal by electrolytes can be minimized when lithium triflate (lithium trifluoromethanesulfonate or LiT) is used as the electrolyte.^{3–5,9}

In previous work²² we used EC/MS to investigate the electrochemical processes that lead to the formation of transient radical cations in the oxidation of triphenylamine (TPA). TPA was used as a model compound in the studies of transient radicals because of its well-characterized electrochemical behavior. An EC cell that was designed for these experiments was coupled via the particle beam (PB) liquid interface to a quadrupole mass spectrometer with an electron impact (EI) ionization ion source.²² In EC/PB-MS experiments with TPA, a molecular ion, TPA^{•+}, at m/z 245, and an ion at m/z 244 were detected. While the ion at m/z 245 was easily assigned to the TPA^{•+} radical cation, the identity of the ion at m/z 244 was more ambiguous. The m/z 244 ion can result from a loss of a hydrogen from TPA^{•+} radical cation (i.e., [TPA^{•+} - H⁺]^{•+}) or may be due to a dication (TPB²⁺) of tetraphenylbenzidine dimer (TPB MW 488), which is a product of the electrochemical oxidation of TPA.²³ The TPA oxidation pathway that was proposed based on the EC/PB-MS results²² and past work²³ is shown in Scheme 1.

In the present work, a new miniaturized EC cell was designed for ESI-MS experiments in which a high-resolution Fourier transform ion cyclotron resonance mass spectrometer (FTICR MS) was used to exploit the high mass resolving power of FTICR

MS in MS detection of the EC reaction products. In this work, the EC/ESI-FTICR MS experiments have demonstrated two identities of the m/z 244 ion that were due to TPB²⁺ dications, when the EC cell voltage was applied, and to [TPA^{•+} - H⁺]^{•+} ions, in the absence of the on-line EC cell voltage. In the FTICR MS experiments, the m/z values of the isotopic ions, and the relative abundances, were used to distinguish the two types of m/z 244 ions. TPB²⁺ ion signal was distinguished from the second harmonic signal of TPB^{•+} ion of the same m/z in separate experiments in which selective ion ejection from the ICR cell was employed.

The ESI-MS and EC/ESI-MS results point to an uneven distribution of the interfacial potential in ESI-MS, along the axial position of the ES needle. This was predicted by Van Berkel and co-workers by computer simulations of the ESI processes. The simulations predict that the electrolytic reactions in the ESI process are confined to the ES tip region.²⁴

In addition, new results are reported, which show that the suppression of the ESI-MS signals by TBAP can be alleviated in EC/ESI-MS. The present work demonstrates the advantages of coupling of an EC cell to ESI-MS for sensitivity enhancement.

EXPERIMENTAL SECTION

Materials. TPA (98%) was from Aldrich (St. Louis, MO) and LiT and TBAP were from Alfa Aesar (Ward Hill, MA). HPLC-grade acetonitrile was from Fisher (Pittsburgh, PA).

(22) Zhang, T.; Brajter-Toth, A. *Anal. Chem.* **2000**, *72*, 2533–2540.

(23) Seo, E. T.; Nelson, R. F.; Fritsch, J. M.; Marcoux, L. S.; Leedy, D. W.; Adams, R. N. *J. Am. Chem. Soc.* **1966**, *3498*–3503.

(24) Van Berkel, G. J.; Giles, G. E.; Bullock, IV, J. S.; Gray, L. J. *Anal. Chem.* **1999**, *71*, 5288–5296.

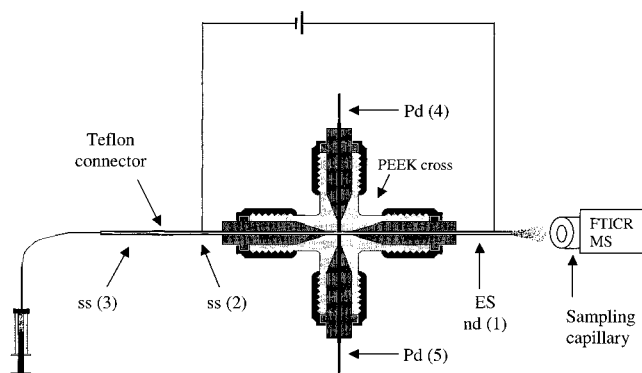


Figure 1. Schematic of the EC flow cell for EC/ESI-FTICR MS. Stainless steel capillaries nd(1), ss(2), and ss(3) and Pd wires Pd(4) and Pd(5) are held in place by a PEEK cross. The ES needle nd(1) is the working electrode in the EC nd(1)–ss(2) cell configuration, in which the positive EC cell voltage is applied to nd(1) as shown.

EC/ESI-FTICR MS. All experiments were conducted with a Bruker APEX 4.7-T FTICR mass spectrometer (Bruker Daltonics, Billerica, MA). An 800 L/s N_2 pump and two 400 L/s cryopumps pumped the FTICR external source housing, the ion-transfer region, and the high-vacuum ($\sim 2 \times 10^{-9}$ mbar) ICR analyzer region, respectively.

A dual-stage ESI source (Analytica of Branford, Branford, CT) was used with a 500 L/min mechanical pump and a turbo-drag pump on the first and second stages, which reduced the pressure from atmospheric to $\sim 5 \times 10^{-3}$ mbar. The ES voltage was 3.3 kV. A 1×10^{-4} M TPA and 2×10^{-4} M electrolyte solution in acetonitrile was delivered by a syringe pump (74900 series, Cole Parmer, Vernon Hills, IL), at 75 μ L/h. The ES stainless steel capillary, nd(1), was a part of the EC flow cell (Figure 1). The dimensions of the electrodes in the EC cell in Figure 1 are as follows: nd(1), 100 μ m i.d., 4 cm long, with a capillary volume of ~ 0.3 μ L; ss(2), 200 μ m i.d., 5.08 cm long; ss(3), 200 μ m i.d., 2.54 cm long; Pd(4) and Pd(5), 1 mm diameter. The distance between the Pd wires that form a liquid gap is ~ 500 μ m. The results that were obtained with the thin-layer Pd(4)–Pd(5) cell configuration are not included in the present work. The PEEK cross (Upchurch Scientific, Oak Harbor, WA) has a swept volume of ~ 0.8 μ L. The total volume, after ss(2), is ~ 1.1 μ L. The EC cell voltage was 7.5 V and was applied from a battery adjustable through a voltage divider and was floated at the ES needle voltage. *Caution: High voltage is hazardous. Care should be taken in performing the experiment.*

A stainless steel sample desolvation capillary (500 μ m i.d. \times 170 mm long) in the ES source, biased at 20 V, was heated to 100 $^{\circ}$ C. The capillary–ES needle distance was 3 mm. A skimmer, biased at 10 V, sampled the ions exiting the heated capillary. The ions were trapped in a hexapole ion transfer/storage region for 0.2 s before transfer to the ICR cell. The pressure after the hexapole was $\sim 2.9 \times 10^{-6}$ mbar. The ions were ejected from the ICR cell by single-frequency resonant irradiation at the ICR frequency corresponding to the selected m/z .

Data Processing. The Bruker Apex FTICR XMASS (version 4.0) program was used to acquire time-domain mass spectra. Broadband detection was used with a mass range of 150–800 amu. Each transient signal was an average of 20 scans unless specified otherwise and was composed of 64K data points. A locally written

program was used to facilitate handling of the time-domain mass spectra. After magnitude mode Fourier transformation, ion peak heights were obtained using the line-listing command of the program and were used to calculate isotopic ratios of the individual ions. The program calculated the theoretical isotope distributions after the formula and charge of each ion were entered. XMASS results are shown with an absolute intensity scale determined by the XMASS program.

RESULTS AND DISCUSSION

EC Cell. A schematic diagram of the EC cell that was used in the EC/ESI-FTICR MS experiments is shown in Figure 1. The design of the cell allowed testing of different two-electrode on-line cell²⁵ configurations under the same MS conditions. For example, the ES needle nd(1) was used as the working, and stainless steel ss(2) as the counter electrode, respectively, to achieve a fast MS response. In this configuration, the ES nd(1) is the positive electrode (anode) and the EC cell voltage is floated at the (high) ES voltage. In the ss(2)–ss(3) EC cell configuration, the positive voltage is applied to the ss(2) working electrode, and the cell voltage is isolated from the ES voltage. The Pd(4)–Pd(5) electrodes produced a thin-layer cell design, while the nd(1)–ss(2) and ss(2)–ss(3) EC cell configurations are of the tubular design. A comparison of the results obtained in the different electrode configurations in the on-line EC cell allowed the investigation of the effect of the EC cell voltage on sensitivity in ESI-MS.

ESI and EC/ESI-MS of TPA. Figure 2a shows an ESI-FTICR MS mass spectrum of TPA. The m/z 245, 412, and 488 ions are due to TPA^{+} , $[TPA + (TPA - C_6H_6)]^{+}$, and TPB^{+} , respectively. The ion assignments were confirmed from the abundance ratios of the isotopic ($M + 1$)/ M ions and are summarized in Table 1. The ions that were detected are formed during the ESI (of neutral TPA) during the electrolytic ESI processes,^{11,16,17} which favor oxidation of compounds with a low oxidation potential. The high signal of TPA^{+} relative to TPB^{+} signal shown in Figure 2a confirms rapid formation of TPA^{+} .²³

Figure 2b shows the EC/ESI-MS mass spectrum of TPA after the EC cell voltage was applied in the nd(1)–ss(2) EC cell configuration, with the electrochemical oxidation occurring in the on-line EC cell at the nd(1) working electrode. As can be seen from the comparison of the results in Figure 2a and b, after the EC cell voltage is applied, a significant enhancement of the TPB^{+} ion signal is observed relative to the TPA^{+} ion signal. As shown in Figure 2c, the enhancement of TPB^{+} ion signal relative to TPA^{+} signal can be achieved in ss(2)–ss(3) EC cell configuration, when the oxidation of TPA occurs at the ss(2) as the working electrode. The intensity ratio of TPB^{+} to TPA^{+} is ~ 0.4 in ESI-MS (Figure 2a), while in EC/ESI-MS the intensity ratio of TPB^{+} to TPA^{+} is ~ 6.2 in nd(1)–ss(2) (Figure 2b) and ~ 7.3 in ss(2)–ss(3) (Figure 2c) EC cell configuration, respectively. The results verify that oxidation of TPA in the EC cell produces the TPB dimer.^{22,23} The yield of the dimer is affected by flow rate, as discussed below. In the tubular EC cell design, under flow conditions of the EC/ESI-MS experiment, reduction at the counter electrode of the oxidation products generated at the working electrode is unlikely. The nature of the counter electrode reactions was not investigated.

(25) Bard, A. J.; Faulkner, L. R. *Electrochemical Methods*; Wiley: New York, 1980.

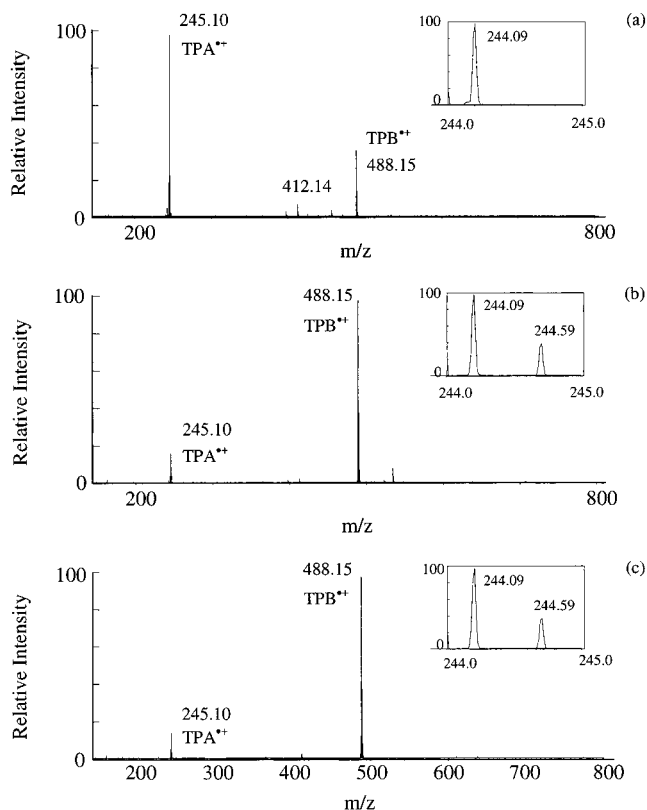


Figure 2. ESI (a) and EC/ESI (b, c) mass spectra of TPA. EC cell configuration: (b) nd(1)–ss(2); (c) ss(2)–ss(3). Conditions: 1×10^{-4} M TPA, 2×10^{-4} M LiT in acetonitrile, flow rate $75 \mu\text{L/h}$, ES voltage 3.3 kV, EC cell voltage 7.5 V, scan range 150–800 amu, and 20 scans.

The results in Figure 2 show that the formation of TPB dimer is limited in ESI-MS. This is consistent with the results of computer simulations, which have predicted a decrease in the ES interfacial potential along the ES needle during the ESI processes.²⁴ In the absence of the EC cell voltage, the formation of TPA^+ is limited to the ES tip and results in limited formation of the TPB^+ ion.

Ion Assignments. The insets in Figure 2 show that the m/z 244.09 ions form in ESI-MS and EC/ESI-MS; an isotopic ion, at m/z 244.59, is only observed in the EC/ESI-MS mass spectra (Figure 2b and c insets). The half-integral m/z separation, which is observed between the isotopic ions, strongly suggests that a doubly charged TPB^{2+} ion is formed in EC/ESI-MS.²² As shown in Table 1, the 36.6% abundance ratio of the TPB^{2+} isotopic ion matches closely that calculated for the m/z 244.59/244.09 ions from the known isotopic abundances. The final assignment of the m/z 244.09 and 244.59 ions as TPB^{2+} was made after the second harmonic ion contribution of TPB^+ to the 244.59/244.09 ion intensity ratio was excluded, as described below. The m/z 244.09 ion, which is detected in ESI-MS without the isotopic m/z 244.59 ion (Figure 2a, inset), was assigned to $[\text{TPA}^+ - \text{H}]^+$. The isotopic ($M + 1$) ion of $[\text{TPA}^+ - \text{H}]^+$ has the same m/z as TPA^+ (m/z 245.10). Because of the interference, the presence of the ($M + 1$) ion of $[\text{TPA}^+ - \text{H}]^+$ is not apparent from the ($M + 1$)/ M isotopic ratio.

In FTICR MS, harmonic signals can be detected together with the fundamental ICR signals.^{26,27} This can interfere with assignments of multiply charged ions because the harmonic and multiply

charged ion signals have the same isotopic distributions. For example, when m/z 488.15 TPB^+ ion is detected by EC/ESI-FTICR MS, the third harmonic signals of this ion are also detected at m/z 162.75 and 163.09. As a result, the assignment of TPB^{2+} ions, which have the same m/z as the second harmonic ions of TPB^+ , required further verification.

Selective ejection from the ICR cell, of ions of a particular m/z , can eliminate the associated harmonic ion signals.^{26,27} In EC/ESI-FTICR MS, TPB^+ is expected to be present because the signal of the dimer is high in EC/ESI-MS. To determine whether the m/z 244.09 and 244.59 ions were due to TPB^{2+} or to the second harmonic signal of TPB^+ , the ions of m/z 488.15 were ejected from the ICR cell. After the ejection, the signals at m/z 488.15, 162.75, and 163.09 disappeared, as expected for signals due to TPB^+ . At the same time, m/z 244.09 and 244.59 ions maintained their intensity, which verified that the TPB^{2+} ions continued to be present in the ICR cell.

Ion Formation in the EC Cell. The changes in the ion intensities of TPA^+ , TPB^+ , and TPB^{2+} ions, and the changes in the corresponding isotopic intensity ratios, with time, after the EC cell voltage was applied, are illustrated in Figure 3. As can be seen from Figure 3a, after the EC cell voltage is applied to the nd(1) and ss(2) electrodes, an increase in TPA^+ ion signal is observed, which decreases with time while the signal of TPB^+ increases; the steady-state signal is rapidly reached. When the EC cell voltage is disconnected, the signals return to their background level. The increase of m/z 244.09 TPB^{2+} ion signal is also observed after the EC cell voltage is applied (Figure 3a), but the steady-state signal of this ion is reached more slowly. The results show that the oxidation of TPA in the EC cell, with formation of TPB^+ is rapid after the EC cell voltage is applied, while the formation of TPB^{2+} is slower. Slow oxidation of TPB^+ to TPB^{2+} has been reported previously.^{23,28–30}

The slow increase of the m/z 244.09 ion signal, after the EC cell voltage is applied, may be a result of a slow formation of TPB^{2+} or may result from a slow formation of $[\text{TPA}^+ - \text{H}]^+$ ions of the same m/z . Similar values of isotopic intensity ratios of m/z 244.59/244.09 ions, and those of m/z 489.14/488.15 of TPB^+ , shown in Figure 3b, which can be expected to be similar, indicate that m/z 244.09 ions are due to TPB^{2+} . The small initial value of the ratio (of m/z 244.59/244.09 ions, Figure 3b) indicates that initially $[\text{TPA}^+ - \text{H}]^+$ ions contribute to the m/z 244.09 ion signal. Isotopic signal of $[\text{TPA}^+ - \text{H}]^+$ ions at m/z of 245.10 is not monitored in the ratios in Figure 3b.

Protonation of TPA in EC/ESI-MS. The increase of the m/z 246.11/245.10 ion ratio with time, after the EC cell voltage is applied, shown in Figure 3b, is consistent with the increase in protonation of TPA to $[\text{TPA} + \text{H}]^+$ (m/z 246.11). $[\text{TPA} + \text{H}]^+$ ions are observed when the ES needle nd(1) functions as the working electrode in the nd(1)–ss(2) on-line EC cell (Figure 3b). The results in Table 1 verify that formation of $[\text{TPA} + \text{H}]^+$ ions is not significant in ESI-MS, in the absence of the EC cell voltage, as indicated by the intensity ratio of m/z 246.11/245.10 ions of

(26) Limbach, P. A.; Schweikhard, L.; Cowen, K. A.; McDermott, M. T.; Marshall, A. G.; Coe, J. Y. *J. Am. Chem. Soc.* **1991**, *113*, 6795–6798.

(27) Grosshans, P. B.; Marshall, A. G. *Int. J. Mass Spectrom.* **1991**, *107*, 49–81.

(28) Nelson, R. F.; Philp, Jr., R. H. *J. Phys. Chem.* **1979**, *83*, 713–716.

(29) Oyama, M.; Ozaki, K.; Okazaki, S. *Anal. Chem.* **1991**, *63*, 1387–1392.

(30) Sumiyoshi, T. *Chem. Lett.* **1995**, 645–646.

Table 1. Calculated and Measured m/z Values of Detected Ions and Corresponding Isotopic Distributions

ion identity	calculated			measured			
	m/z		isotopic ratio, % (M + 1)/M	m/z		isotopic ratio, %	
	M	M + 1		M	M + 1	(M + 1)/M ESI	(M + 1)/M EC/ESI ^a
[TPA - H] ⁺	244.11	245.12	20.6	244.09	245.10	1500 ^b	450 ^b
TPB ²⁺	244.11	244.61	41.2	244.09	244.59	nd ^c	36.6
TPB ^{•+}	488.22	489.23	41.2	488.15	489.14	38.6	38.6
TPA ^{•+}	245.12	246.12	20.7	245.10	246.11	23.0	31.1
(TPB - C ₆ H ₄) ^{•+}	412.19	413.20	34.4	412.14	413.15	33.0	33.4
TBA ^{•+}	242.28	243.29	18.7	242.26	243.28	17.5	16.9

^a EC cell voltage 7.5 V, nd(1)–ss(2) EC cell configuration. ^b Unreasonably high value due to spectral overlap of the peaks due to isotopic (M + 1) ion of [TPA^{•+} - H]⁺ and TPA^{•+} at m/z 245.10. ^c nd, not detected.

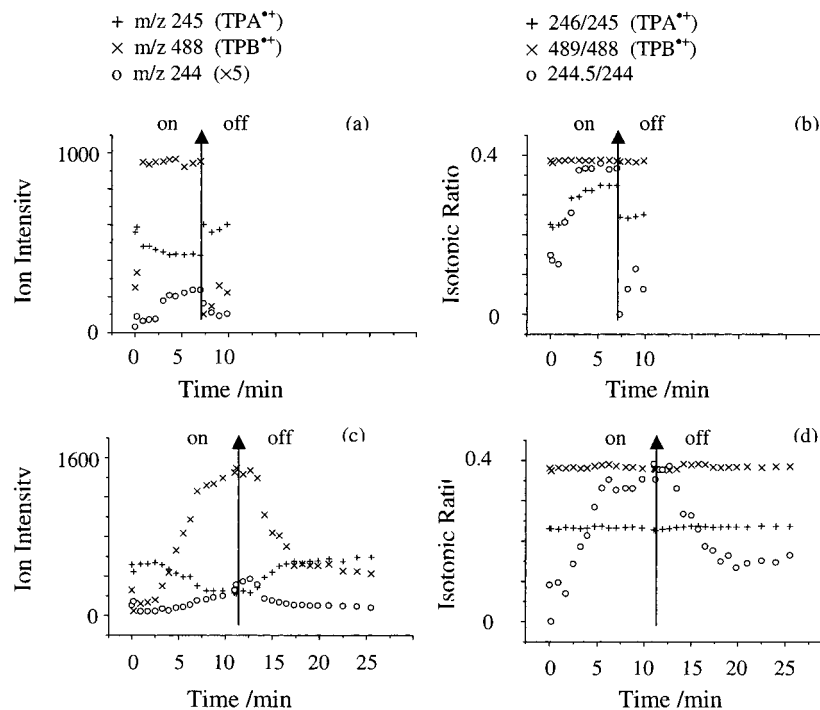


Figure 3. Ion intensities (a, c) and isotopic intensity ratios (b, d) in EC/ESI-MS during (on) and after (off) application of the EC cell voltage. EC cell configuration: (a, b) nd(1)–ss(2); (c, d) ss(2)–ss(3). Conditions as in Figure 2. Each data point represents one measurement. The data have been reproduced three times with deviation below 10%.

23.0%, which is close to that expected for the TPA isotopic abundance ratio (20.7%). The m/z 246.11/245.10 ion ratio increases to 31.1% in EC/ESI-MS, supporting formation of [TPA + H]⁺, when the EC cell voltage is applied.

Protonation of TPA may be related to an increase in ESI current, which is observed after the EC cell voltage is applied to the nd(1)–ss(2) on-line EC cell. The ES current is more stable when the EC cell voltage is applied, possibly because it is larger. In a stable ES process, the ES current has to be equal in magnitude, based on charge balance considerations, to the faradaic electrolysis current at the ES metal/solution interface.^{11,16,17} The actual redox reactions during the electrolysis, and the extent to which they occur during the ES ionization, are determined by redox potentials, and the relative concentrations of species, which can include capillary metal, analytes, water, and the solution impurities.¹⁷ The high ESI current that is observed when the EC cell voltage is applied may be due to higher ion concentrations, as a result of electrochemical reactions in the EC cell. The increase in the ESI current can enhance electrolysis at

the ES metal/solution interface, which may result in more extensive oxidation of the analyte solution. As a result oxidation of water may occur, which can decrease the solution pH, favoring protonation of TPA.³¹ The labeled water content of the HPLC-grade acetonitrile is 0.002%, which is ~ 0.9 mM. It is reasonable to assume that the concentration of water impurity in TPA–acetonitrile solution is at the literature-reported level, ~ 4 –10 mM;³² the moisture level may increase during the atmospheric ESI process.

The basicity of amines is structure dependent,³³ and as a result, aromatic amines are weak bases when compared with ammonia or aliphatic amines. Aniline has a pK_a of 4.58 and TPA can be expected to be a weaker base because of resonance stabilization. As a result, TPA cannot be considered basic.³³ However, oxidation

(31) Van Berkel, G. J.; Zhou, F. M.; Aronson, J. T. *Int. J. Mass Spectrom. Ion Processes* **1997**, 162, 55–67.

(32) Adams, R. N. *Acc. Chem. Res.* **1969**, 2, 175–180.

(33) Barton, D.; Ollis, W. D. *Comprehensive Organic Chemistry: the Synthesis and Reactions of Organic Compounds*; Oxford Pergamon Press: New York, 1979.

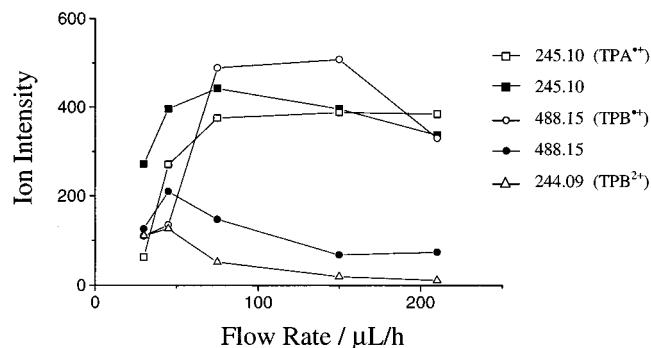


Figure 4. Ion signals as function of flow rate in ESI-MS (solid) and EC/ESI-MS (open). TPA⁺ (square), TPB⁺ (circle), and TPB²⁺ (triangle). EC/ESI-MS data at steady state, ~3 min after the EC cell voltage was applied. Conditions as in Figure 2.

of water may cause a decrease in the solution pH, facilitating protonation of TPA. The intensity ratio of m/z 246.11/245.10 ions in ESI-MS is close to that expected from the isotopic abundance ratio of unprotonated TPA, indicating that the oxidation of water is limited to EC/ESI-MS.

EC/ESI-MS with the ss(2)–ss(3) Electrodes. The ss(2)–ss(3) EC cell configuration was tested in EC/ESI-MS, with ss(2) as the working and ss(3) as the counter electrode, respectively. In this configuration, the EC cell voltage is isolated by the polyetheretherketone (PEEK) cross from the ESI voltage. In this electrode configuration, the ion signals of TPA⁺, TPB⁺, and TPB²⁺ ions (Figure 3c and d) are similar to the signals that were detected in EC/ESI-MS with the ES nd(1) as the working and ss(2) as the counter electrode (Figure 3a and b). The results in Figure 3 show that the ions are detected more slowly when the ss(2)–ss(3) EC cell configuration is used. This is consistent with the greater distance of the working ss(2) electrode to the ESI ion source. No obvious protonation of TPA is observed when the ss(2)–ss(3) EC cell configuration is used in EC/ESI-MS as evidenced by the constant (~23.0%) intensity ratio of m/z 246.11/245.10 ion signals (Figure 3d). The absence of apparent protonation is consistent with lower ESI currents in this electrode configuration.

Effect of Flow Rate. Figure 4 shows the effect of flow rate on the relative signal intensities of TPA⁺, TPB⁺, and TPB²⁺ ions. The results in Figure 4 show that the detection sensitivity can be improved by EC/ESI-MS and by optimizing the flow rate. For example, TPA⁺ and TPB⁺ ion signals are high at higher flow rates, above 100 $\mu\text{L/h}$, in EC/ESI-MS (open symbols). TPB⁺ signal is significantly higher in EC/ESI-MS than in ESI-MS at flow rates greater than 50 $\mu\text{L/h}$. TPB²⁺ signal can be detected (in EC/ESI-MS only) with good sensitivity at low flow rates below 45 $\mu\text{L/h}$.

It is of interest that in EC/ESI-MS new ions at m/z 487.14, 486.13, 485.12, and 484.12 were observed at very low flow rates of 30 $\mu\text{L/h}$ (Figure 5). The ions may form from TPB⁺ (m/z 488.15) by hydrogen loss. The loss of hydrogen from cations in the gas phase is known.³⁴ The ions at m/z 486.13, 485.12, and 484.12 may result from repetitive loss of either H⁺ or H₂ from the ions of m/z 487.14 or 488.15; no attempt was made to identify the ion formation pathways.

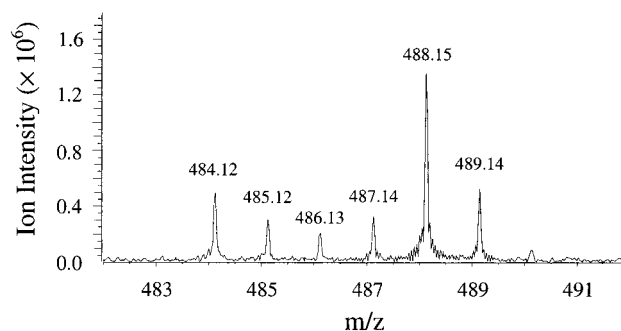


Figure 5. EC/ESI-MS of TPB⁺ and related ions at low flow rates (30 $\mu\text{L/h}$). Bruker XMASS intensity scale.

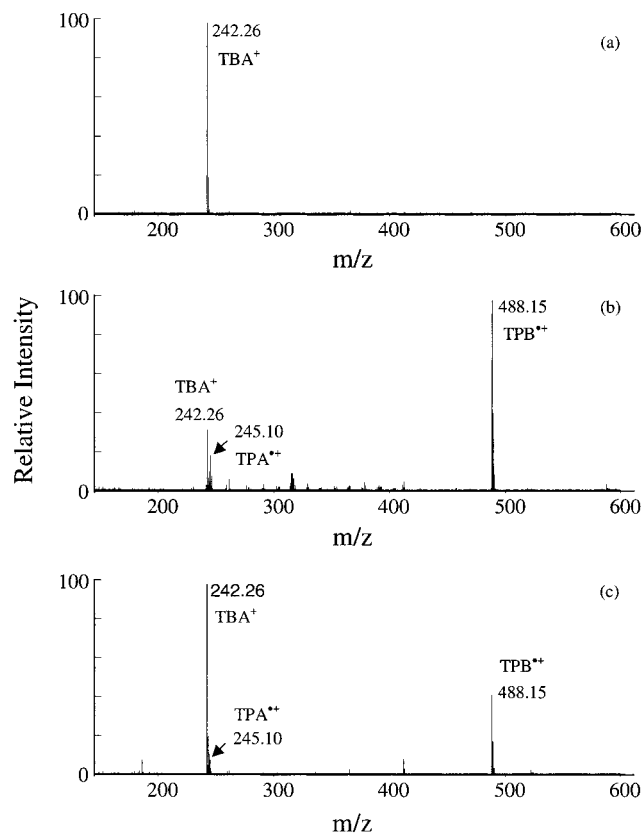


Figure 6. ESI-MS (a) and EC/ESI-MS (b, c) mass spectra of TPA with TBAP. EC cell configuration: (b) nd(1)–ss(2); (c) ss(2)–ss(3). Conditions: 1×10^{-4} M TPA, 2×10^{-4} M TBAP in acetonitrile, flow rate 75 $\mu\text{L/h}$, ES voltage 3.0 kV, EC cell voltage 7.5 V, scan range 150–800 amu, and 5 scans.

Limited Signal Suppression by TBAP in EC/ESI-FTICR MS. The presence of electrolytes is required in the electrochemical experiments to sustain the EC cell current. In EC/ESI-MS, however, electrolyte can contribute to the suppression of ESI-MS signal of analytes.^{2,3,19–21} Signal suppression in the presence of electrolytes such as TBAP and Bu₄NPF₆ is a consequence of effective competitive emission of electrolyte ions in the presence of analyte ions. TBAP and Bu₄NPF₆ are surface-active; emission of the electrolyte ions is efficient in ESI even at low electrolyte concentrations.^{2,3} With lithium triflate, which is less surface-active than TBAP and Bu₄NPF₆, signal suppression in EC/ESI-MS is less.^{2–5,9} To enhance the efficiency of EC/ESI-MS in the presence of Bu₄NPF₆, off-line bulk electrolysis was investigated by Bond and co-workers.² With an EC cell operated at ~200 V using a

(34) Guo, X.; Sievers, H. L.; Grutzmacher, H. F. *Int. J. Mass Spectrom.* **1999**, *185*, 1–10.

fused-silica ES capillary, the electrochemical reaction products were detected in the presence of Bu_4NPF_6 .

In this work, the electrolyte signal of TBA^+ was observed in ESI-MS and the signal of TPA was not detected (Figure 6a) when a stainless steel ES capillary was used. However, after the EC cell voltage was applied, the signal of TPA (and TPB) was detected while the signal of TBA^+ decreased (Figure 6b). Similar results, in terms of the ratio of TPB^{2+} versus TPA^{2+} ion signals in the presence of TBAP were observed in nd(1)–ss(2) and ss(2)–ss(3) EC cell configurations (Figure 6c).

The EC/ESI-MS results in Figure 6 indicate that reactions in the EC cell contribute to the efficiency of ion formation, which results in high EC/ESI-MS sensitivity and limits signal suppression by TBAP. Consequently, the results that were obtained with TBAP and lithium triflate as electrolytes are similar (Figures 2 and 6). The sensitivity is highest with the ES needle nd(1) as the working electrode (Figure 6b).

CONCLUSIONS

A new EC cell was designed and coupled to an ESI-FTICR MS. The high mass resolving power and ion ejection capability of FTICR MS was exploited to determine two identities of the m/z 244 ions that originated from TPA. The ions were identified as TPB^{2+} with the EC cell-on and $[\text{TPA}^{2+} - \text{H}]^+$, with the cell-off. Ion signals of TPA^{2+} , TPB^{2+} , and TPB^{2+} ions were enhanced in EC/ESI-MS; the relative signal enhancement was a function of flow rate. The EC/ESI-MS results indicate fast formation of TPB^{2+} and slow generation of TPB^{2+} . The increased reaction time in the

EC cell at low flow rates favors formation of TPB^{2+} ions. At low flow rates, new ions that may form as a result of hydrogen loss from TPB^{2+} were detected.

The ESI-MS and EC/ESI-MS results provide evidence of an uneven distribution of interfacial potentials along the ES needle in ESI-MS. As a result, in the absence of the EC cell voltage, electrolytic oxidation in ESI-MS is confined to the ES tip, and the ion formation efficiency is lower than in EC/ESI-MS. In EC/ESI-MS in the nd(1)–ss(2) EC cell configuration, with the ES needle as the working electrode, high ES current is observed. Under these conditions, protonation of TPA is observed. Electrolytic oxidation of water, which may occur to support the increase in the ES current after the EC cell voltage is applied in EC/ESI-MS, can result in a decrease in solution pH, contributing to the protonation of TPA.

It is demonstrated that the signal suppression problem in the presence of TBAP electrolyte can be alleviated in EC/ESI-MS at low EC cell voltage. The nd(1)–ss(2) EC cell configuration, with the ES needle as the working electrode, is advantageous in terms of fast response and high MS sensitivity and is found to be advantageous in limiting signal suppression by surface-active TBAP.

Received for review June 25, 2001. Accepted December 5, 2001.

AC015543L